JACS
JOURNAL OF THE AMERICAN CHEMICAL SOCIETY
Cite This: J. Am. Chem. Soc. XXXX, XXX, XXX−XXX
Communication
pubs.acs.org/JACS

Mechanistic Studies of Proton-Coupled Electron Transfer in a Calorimetry Cell

Fangfang Zhong and Ekaterina V. Pletneva*

Department of Chemistry, Dartmouth College, Hanover, New Hampshire 03755, United States

Supporting Information

ABSTRACT: Mechanistic studies of proton-coupled electron-transfer (PCET) reactions in proteins are complicated by the challenge of following proton transfer (PT) in these large molecules. Herein we describe the use of isothermal titration calorimetry (ITC) to establish proton involvement in protein redox reactions and the identity of PT sites. We validate this approach with three variants of a heme protein cytochrome *c* (cyt *c*) and show that the method yields a wealth of thermodynamic information that is important for characterizing PCET reactions, including reduction potentials, redox-dependent pK_a values, and reaction enthalpies for both electron-transfer (ET) and PT steps. We anticipate that this facile and label-free ITC approach will find widespread applications in studies of other redox proteins and enhance our knowledge of PCET reaction mechanisms.

Proton-coupled electron-transfer (PCET) reactions are central to biological redox processes[1,2] and also underlie the action of many chemical systems for energy conversion in small-molecule catalysis, electrochemical devices, and solar cells.[3−5] Mechanistic investigations of PCET in proteins have illustrated the exquisite control of PCET reactivity in these native systems[1,2,6−8] and the value of studying them directly, both to uncover the details of biological mechanisms and to guide the design of bioinspired chemical systems.

Tracking protonation changes and even determining whether proton transfer (PT) accompanies the redox change in proteins, however, can be difficult. The pH dependence of the reduction potential is a useful marker of PCET behavior, but these measurements can be complicated by difficulties in establishing protein−electrode interactions, the use of mediators, and the presence of multiple redox centers. The pH dependence of rates of redox reactions is commonly measured in PCET studies, but its origin has been debated.[9] NMR and IR measurements are traditionally used to identify the ionizable groups,[10−12] but obtaining this information for proteins is complicated by the many titratable groups and spectral overlap.

We have developed a method to perform proton inventory and determine sites of protonation (deprotonation) in redox reactions. Isothermal titration calorimetry (ITC) is a powerful tool to get access to the protonation equilibria and redox thermodynamics. Inspired by proton-linkage studies of protein−protein complexation,[13−15] we thought that when redox reactions are performed through isothermal titrations in a calorimetry cell,[16] associated changes in the observed (apparent) enthalpy (ΔH_{obs}) can be used to determine the number of protons involved and the sites of protonation (deprotonation). When redox reactions are accompanied by protonation (deprotonation) processes, the observed calorimetric enthalpy of the reaction (ΔH_{obs}) will depend on the buffer ionization enthalpy (ΔH_{ion}) and the protonation enthalpy of the ionizable group (ΔH_{prot}) scaled by the number of protons involved (Δn_{H+}) (eq 1, where ΔH_0 is the enthalpy of the reaction in a buffer with zero ionization enthalpy).[15,17] The pK_a values and site-specific enthalpies of protonation ΔH_{prot} can be extracted from measurements of apparent enthalpies ΔH_{obs} at different pH and in buffers that differ in ΔH_{ion}. Importantly, different ionizable groups in proteins have distinct ΔH_{prot} values (Table S1),[15,17−19] and these parameters, together with pK_a values, can be used to identify (or narrow down) the groups involved.

$$\Delta H_{obs} = \Delta H_{rxn} + \Delta n_{H+} \times (\Delta H_{ion} + \Delta H_{prot}) = \Delta H_0 + \Delta n_{H+} \times \Delta H_{ion} \quad (1)$$

We have validated this protocol with pseudowild-type (WT*) and two switchable variants of yeast *iso*-1 cyt *c* (Figure 1 and Figure S1).[20] Redox-linked ligand switching of K79H[21,22] and T78C/K79G[23] was expected to be coupled with deprotonation of His and Cys side chains, respectively, under some pH conditions. Work by Bowler et al. on K79H[24] and our studies of T78C/K79G (Figure S2) demonstrate that the kinetics of redox reactions for both of these variants indeed depend on pH. Analyses of these kinetics have revealed intrinsic $pK_a^{int,ox}$ values (Table 1) for ferric (oxidized) species consistent with deprotonation of His and Cys. The 695 nm charge-transfer band is a characteristic feature of the Fe(III)-Met ligation in cyt *c*.[25] At fast bimolecular oxidation rates, this band is readily apparent in spectra of early reaction transients for both K79H and T78C/K79G (Figure S3), suggesting that electron transfer (ET) precedes the ligand switch (Scheme 1).

Figure 2 depicts redox processes and coupled protonation and ligand-switching equilibria in K79H and T78C/K79G. The pK_a values for deprotonation of XH^+ (His79 and Cys78 here) in ferric proteins (pK_a^{ox}) are sums of $pK_a^{int,ox}$ and pK_C (eq 2),[26] where K_C is a conformational exchange constant related to the difference in stability of Met80- and X-ligated conformers (Scheme S1). Since there is no ligand switch in ferrous proteins, $pK_a^{int,red} = pK_a^{red}$. Fractional populations of

Received: April 1, 2019
Published: June 9, 2019

DOI: 10.1021/jacs.9b03512
J. Am. Chem. Soc. XXXX, XXX, XXX−XXX

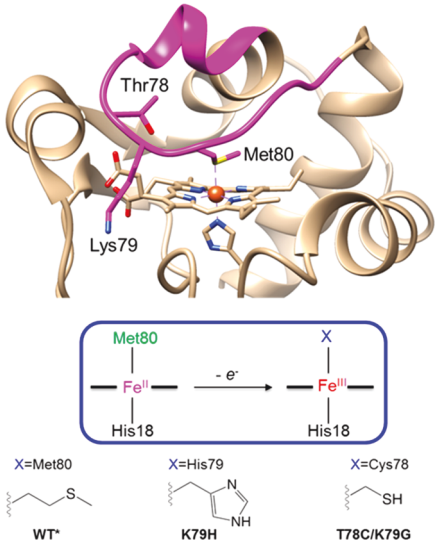

Figure 1. Structure of yeast *iso*-1 cyt *c* showing positions of axial ligand Met80 and mutation sites for variants in this study. In WT*, both ferric and ferrous hemes are Met80-ligated. Ferric K79H undergoes a pH-dependent Met80-to-His79 ligand switch (pK_a^{ox} = 6.03 ± 0.09, ref 21. Ferric T78C/K79G maintains Cys78 coordination to the heme iron over a wide pH range, ref 23. Ferrous K79H and T78C/K79G have Met80 coordinated to the heme iron.

protonated XH^+ species in the ferric (x_{ox}) and ferrous (x_{red}) proteins are defined by eqs 3 and 4, and their difference is Δn_{H+} (eq 5). Reaction enthalpies for heme iron oxidation $\Delta H^{M\text{-}M}$ (without ligand switch) and $\Delta H^{M\text{-}X}$ (with ligand switch) are buffer- and protonation-independent. These values, as well as the enthalpy of protonation ΔH_{prot} of X and the enthalpy of $Co(phen)_3^{3+}$ reduction $\Delta H(Co^{3+/2+})$, are combined with x_{ox} and x_{red} to give ΔH_0 (eq 6).

$$pK_a^{ox} = pK_a^{int,ox} + pK_C \quad (2)$$

$$x_{ox} = \frac{10^{(pK_a^{ox}-pH)}}{1 + 10^{(pK_a^{ox}-pH)}} \quad (3)$$

$$x_{red} = \frac{10^{(pK_a^{red}-pH)}}{1 + 10^{(pK_a^{red}-pH)}} \quad (4)$$

$$\Delta n_{H+} = (x_{ox} - x_{red}) \quad (5)$$

$$\Delta H_0 = \Delta H^{M\text{-}X} + (\Delta H^{M\text{-}M} - \Delta H^{M\text{-}X}) \times x_{ox} + \Delta H_{prot} \times \Delta n_{H^+} + \Delta H(Co^{3+/2+}) \quad (6)$$

Ferrous Met-ligated WT* and mutant cyt *c* proteins were oxidized by titrations with $Co(phen)_3^{3+}$. Experimental thermograms, together with the known thermodynamic values for the

Scheme 1. Redox-Linked Ligand Switching in K79H and T78C/K79G

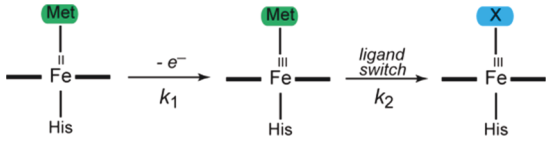

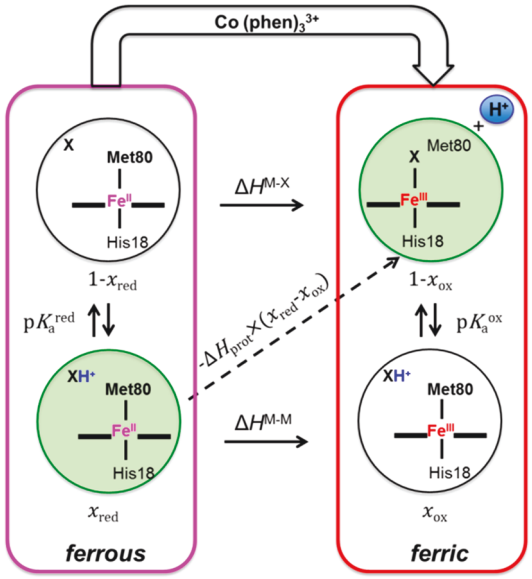

Figure 2. Square scheme showing redox interconversions and the linked ligand-switch and protonation processes in K79H (X = His79) and T78C/K79G (X = Cys78). The dashed arrow represents redox-linked deprotonation of XH^+, and this PCET reaction is stepwise (Scheme 1) and *not* concerted ET/PT.

metal complex,[27] allow for straightforward calculations of heme iron reduction potentials (Figure 3 and Table 2). While ΔH_{obs} for the two switchable mutants show the marked dependence on ΔH_{ion} of buffer at pH 6.0, the ΔH_{obs} values for WT* do not vary with ΔH_{ion} under these conditions (Figure S4). These findings indicate that oxidation of K79H and T78C/K79G results in proton release to the buffer but oxidation of WT* does not. The number of protons Δn_{H^+} and buffer-independent ΔH_0 values extracted from these dependences are listed in Table 2. Our ITC-derived thermodynamic parameters for heme iron reduction are in accord with those from electrochemistry experiments for these and similarly ligated cyt *c* variants (Table S2).[23,27−30]

Extending these measurements to a range of pH has yielded the dependence of Δn_{H+} on pH. For K79H, a variant that is Met-ligated in its ferric state at low pH but becomes His-ligated at high pH (Figure 2), the profile is bell-shaped and both pK_a^{ox} and pK_a^{red} can be extracted from a fit of the

Table 1. pK_a Values and Enthalpies of Heme Iron Oxidation ($\Delta H^{M\text{-}M}$ and $\Delta H^{M\text{-}X}$) and Protonation (ΔH_{prot}) for K79H and T78C/K79G Variants of Yeast *iso*-1 Cyt *c*

variant	X	$pK_a^{int,ox}$[a]	pK_a^{ox}	pK_a^{red}	$\Delta H^{M\text{-}M}$ (kcal/mol)	$\Delta H^{M\text{-}X}$ (kcal/mol)	ΔH_{prot} (kcal/mol)
K79H	His79	6.79 ± 0.06[b]	6.00 ± 0.08[c]	7.19 ± 0.08	16.8 ± 3.1	18.5 ± 1.9	−9.3 ± 2.6
T78C/K79G	Cys78	7.9 ± 0.7	≤2.5[d]	9.7 ± 0.3[e]	15.6 ± 0.9[f]	14.3 ± 4.6	−11.2 ± 5.2

[a] $pK_a^{int,ox}$ is an intrinsic pK_a value (Scheme S1), determined in kinetics studies. [b] From ref 21. [c] pK_a^{ox} = 6.03 ± 0.09, determined from spectrophotometric titrations (ref 21). [d] From ref 23, the value represents the upper limit of pK_a^{ox} since ferric T78C/K79G denatures before Cys78 is protonated. [e] pK_a^{ox} = 2.5 was fixed. [f] The value $\Delta H^{M\text{-}M}$ for WT* was employed.

DOI: 10.1021/jacs.9b03512
J. Am. Chem. Soc. XXXX, XXX, XXX−XXX

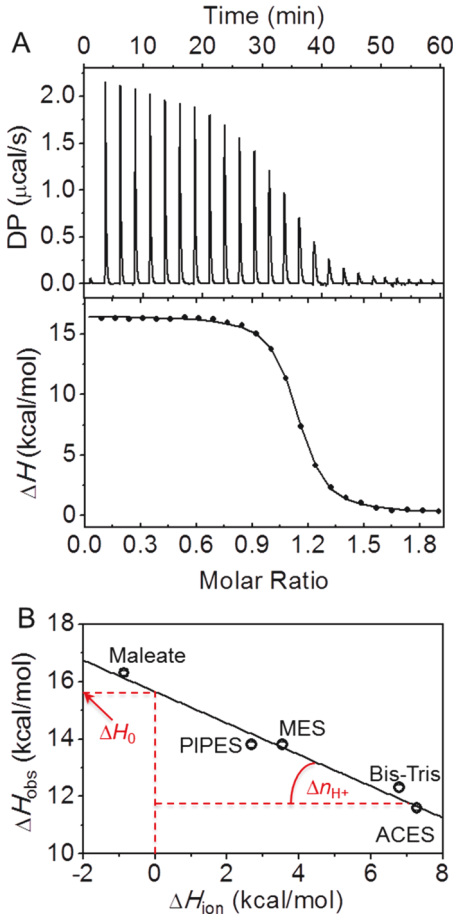

Figure 3. (A) ITC thermogram for oxidation of ferrous K79H by $Co(phen)_3^{3+}$ in a 10 mM maleate buffer at pH 6.25 containing 100 mM NaCl. (B) Dependence of ΔH_{obs} on ΔH_{ion} for oxidation of ferrous K79H by $Co(phen)_3^{3+}$ at pH 6.25. The linear fit of this dependence to eq 1 determines Δn_{H+} (slope) and ΔH_0 (intercept).

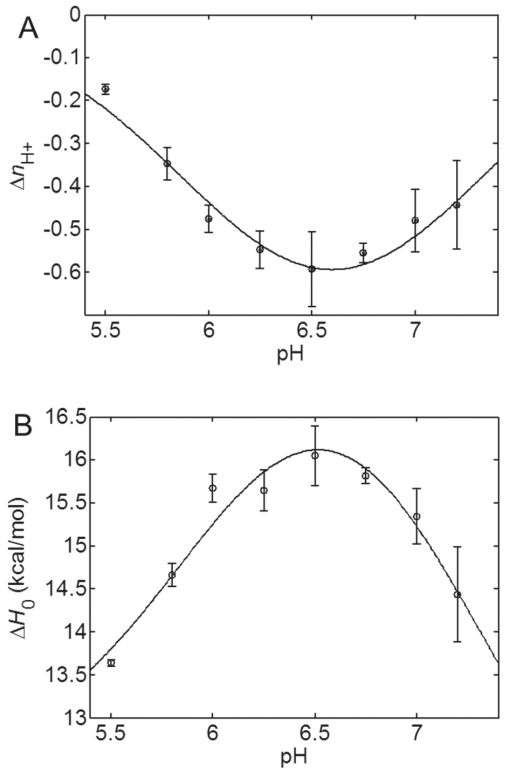

Figure 4. pH dependence of (A) Δn_{H^+} and (B) ΔH_0 for oxidation of ferrous K79H by $Co(phen)_3^{3+}$.

dependence to eq 5 (Figure 4A). The pK_a^{ox} value is similar to that from equilibrium spectroscopic measurements of K79H.[21] For ferric K79H, the comparison of $pK_a^{int,ox}$ and pK_a^{ox} (Table 1) suggests that the His79-ligated conformer is more stable than the Met80-ligated conformer. This relationship can be in part attributed to the higher affinity of ferric heme iron for His than for Met.[21,31]

The pK_a^{red} of K79H has not been known prior to this work. This value is higher than the $pK_a^{int,ox}$ suggesting extra stabilization of the His79-protonated conformer over the deprotonated one upon reduction of the protein. Favorable interactions of the protonated His79 with one of the heme propionates in ferrous K79H (Figure S5A) provide a possible rationale for this result. Analyses of the effects of pH on thermal denaturation of ferrous K79H further support the stabilization effect of His79 protonation (Figure S5B).

Ferric T78C/K79G remains Cys-ligated within the entire pH range studied; ligand displacement in this variant requires highly acidic conditions that result in protein denaturation.[23] This limitation does not allow for independent experimental determination of pK_a^{ox} and, as expected, the ITC-derived pH-dependent redox profile for this variant shows a variation of Δn_{H^+} with pH only at high pH (Figure S6). The acid unfolding results, however, allow us to set the upper limit of pK_a^{ox} (Table 1). Fitting the dependence in Figure S6 with $pK_a^{ox} = 2.5$ yields $pK_a^{red} = 9.7 \pm 0.3$. The finding that $pK_a^{red} > pK_a^{int,ox}$ reveals redox-dependent changes in relative stability of protein conformers with protonated and deprotonated Cys78 in T78C/K79G as well. The interior location of Cys78 in T78C/K79G (Table S3) will favor the protonated (neutral) form of this residue near the ferrous porphyrin.

Analyses of the pH profile of ΔH_0 (Figure 4B and Figure S6B) provide additional pieces of information about the proton-coupled redox reactions in these variants. Fitting these

Table 2. Number of Protons Δn_{H+} and Buffer-Independent ΔH_0 Values for Oxidation by $Co(phen)_3^{3+}$, Heme Iron Reduction Potentials, and Enthalpies of Heme Iron Reduction for Yeast *iso*-1 Cyt *c* Variants from ITC Experiments at pH 6.0

		His18-Fe^{II}-Met80 + $Co(phen)_3^{3+}$ → His18-Fe^{III}-X + $Co(phen)_3^{2+}$		His18-Fe^{III}-X + e^- → His18-Fe^{II}-Met80	
variant	X	Δn_{H+} [a]	ΔH_0 (kcal/mol) [a]	E (mV) [b]	ΔH (kcal/mol) [c]
WT*	Met80	0.04 ± 0.02	7.7 ± 0.1	293 ± 3	−15.6 ± 0.9
K79H	His79	−0.48 ± 0.03	15.7 ± 0.2	246 ± 2	−19.1 ± 1.6
T78C/K79G	Cys78	−0.89 ± 0.04	16.0 ± 0.1	93 ± 3	−13.9 ± 4.7

[a]The data and fits are displayed in Figure S4. [b]Calculated from equilibrium constants (K_{eq}) for the ITC-run oxidation reactions. [c]Calculated as $\Delta H(Co^{3+/2+}) + \Delta n_{H+} \times \Delta H_{prot} - \Delta H_0$. The enthalpy $\Delta H(Co^{3+/2+})$ was taken as −7.9 ± 0.9 kcal/mol, calculated from E and $\Delta S°$ values in ref 27.

DOI: 10.1021/jacs.9b03512
J. Am. Chem. Soc. XXXX, XXX, XXX−XXX

dependences to eq 6 yielded the reaction enthalpies, $\Delta H^{M\text{-}M}$ and $\Delta H^{M\text{-}X}$ as well as the enthalpy of protonation ΔH_{prot} of the PT site (Table 1). The $\Delta H^{M\text{-}M}$ and $\Delta H^{M\text{-}X}$ values are similar, and this finding agrees with the previously suggested importance of entropic factors to the redox change at the heme iron and the ligand-switching mechanism.[29] Importantly, for both K79H and T78C/K79G, ΔH_{prot} is fully consistent with the values for His and Cys (Table S1),[19] respectively, providing an independent confirmation of these groups as the PT site in PCET reactions of these proteins.

In summary, our studies illustrate the utility of ITC as a facile and label-free method to determine proton involvement in redox reactions and the identity of PT sites. The method yields a wealth of thermodynamic information important for characterization of PCET reactions, including reduction potentials, redox-dependent pK_a values, and reaction enthalpies for both ET and PT steps. Our findings with the three cyt *c* variants used to validate this approach are fully consistent with other characterization methods from studies by others or performed in this work. Further, new kinetic data and redox-dependent pK_a values for K79H and T78C/K79G have uncovered properties of conformers involved in redox-linked ligand switching,[32−35] a mechanism common to biological sensors and redox metalloenzymes. We anticipate that this ITC method will find exciting applications in studies of PCET reactions of other metalloproteins, including those where thermodynamic information about ET and PT sites might be difficult to obtain by other means.

■ ASSOCIATED CONTENT

Supporting Information

The Supporting Information is available free of charge on the ACS Publications website at DOI: 10.1021/jacs.9b03512.

Materials and methods; two schemes showing studied equilibria; three tables listing ΔH_{prot} values of protein groups, reduction thermodynamics from electrochemistry, and solvent accessible areas of Cys78 and His79 in modeled conformers; seven figures showing structures of WT, K79H, and T78C/K79G; kinetics of absorption changes upon oxidation of ferrous T78C/K79G by $Co(phen)_3^{3+}$ and pH dependence of k_2; kinetics of absorption changes upon oxidation of ferrous K79H and T78C/K79G by $Fe(CN)_6^{3-}$; plots of ΔH_{obs} versus ΔH_{ion} for WT*, K79H, and T78C/K79G; His79-propionate interactions and pH dependence of T_m for ferrous WT* and K79H; pH dependence of Δn_{H^+} and ΔH_0 for T78C/K79G; and ITC results for oxidation of T78C/K79G by $Ru(NH_3)_6^{3+}$ (PDF)

■ AUTHOR INFORMATION

Corresponding Author

*ekaterina.pletneva@dartmouth.edu

ORCID

Fangfang Zhong: 0000-0002-8168-6424

Ekaterina V. Pletneva: 0000-0003-1380-2929

Notes

The authors declare no competing financial interest.

■ ACKNOWLEDGMENTS

We thank Dean Wilcox for access to his calorimeters and many helpful discussions and Jason Toffey for his contributions during the initial stages of this work. We are grateful to Bruce Bowler for sharing with us the Rbs(WT*) plasmid. This study was supported by NSF Grant CHE-1708592 (E.V.P).

■ REFERENCES

(1) Dempsey, J. L.; Winkler, J. R.; Gray, H. B. Proton-coupled electron flow in protein redox machines. *Chem. Rev.* **2010**, *110*, 7024−7039.

(2) Migliore, A.; Polizzi, N. F.; Therien, M. J.; Beratan, D. N. Biochemistry and theory of proton-coupled electron transfer. *Chem. Rev.* **2014**, *114*, 3381−3465.

(3) Hammes-Schiffer, S. Proton-coupled electron transfer: moving together and charging forward. *J. Am. Chem. Soc.* **2015**, *137*, 8860−8871.

(4) Cukier, R. I.; Nocera, D. G. Proton-coupled electron transfer. *Annu. Rev. Phys. Chem.* **1998**, *49*, 337−369.

(5) Warren, J. J.; Mayer, J. M. Moving protons and electrons in biomimetic systems. *Biochemistry* **2015**, *54*, 1863−1878.

(6) Minnihan, E. C.; Nocera, D. G.; Stubbe, J. Reversible, long-range radical transfer in *E. coli* class Ia ribonucleotide reductase. *Acc. Chem. Res.* **2013**, *46*, 2524−2535.

(7) Hu, S.; Sharma, S. C.; Scouras, A. D.; Soudackov, A. V.; Carr, C. A. M.; Hammes-Schiffer, S.; Alber, T.; Klinman, J. P. Extremely elevated room-temperature kinetic isotope effects quantify the critical role of barrier width in enzymatic C−H activation. *J. Am. Chem. Soc.* **2014**, *136*, 8157−8160.

(8) Edwards, S. J.; Soudackov, A. V.; Hammes-Schiffer, S. Analysis of kinetic isotope effects for proton-coupled electron transfer reactions. *J. Phys. Chem. A* **2009**, *113*, 2117−2126.

(9) Hammes-Schiffer, S. Theory of proton-coupled electron transfer in energy conversion processes. *Acc. Chem. Res.* **2009**, *42*, 1881−1889.

(10) André, I.; Linse, S.; Mulder, F. A. A. Residue-Specific pKa Determination of Lysine and Arginine Side Chains by Indirect 15N and ^{13}C NMR Spectroscopy: Application to apo Calmodulin. *J. Am. Chem. Soc.* **2007**, *129*, 15805−15813.

(11) Zscherp, C.; Schlesinger, R.; Tittor, J.; Oesterhelt, D.; Heberle, J. *In situ* determination of transient pK_a changes of internal amino acids of bacteriorhodopsin by using time-resolved attenuated total reflection Fourier-transform infrared spectroscopy. *Proc. Natl. Acad. Sci. U. S. A.* **1999**, *96*, 5498.

(12) Grytsyk, N.; Sugihara, J.; Kaback, H. R.; Hellwig, P. pK_a of Glu325 in LacY. *Proc. Natl. Acad. Sci. U. S. A.* **2017**, *114*, 1530−1535.

(13) Gómez, J.; Freire, E. Thermodynamic mapping of the inhibitor site of the aspartic protease endothiapepsin. *J. Mol. Biol.* **1995**, *252*, 337−350.

(14) Baker, B. M.; Murphy, K. P. Evaluation of linked protonation effects in protein binding reactions using isothermal titration calorimetry. *Biophys. J.* **1996**, *71*, 2049−2055.

(15) Xie, D.; Gulnik, S.; Collins, L.; Gustchina, E.; Suvorov, L.; Erickson, J. W. Dissection of the pH dependence of inhibitor binding energetics for an aspartic protease: direct measurement of the protonation states of the catalytic aspartic acid residues. *Biochemistry* **1997**, *36*, 16166−16172.

(16) Sørlie, M.; Chan, J. M.; Wang, H.; Seefeldt, L. C.; Parker, V. D. Elucidating thermodynamic parameters for electron transfer proteins using isothermal titration calorimetry: application to the nitrogenase Fe protein. *JBIC, J. Biol. Inorg. Chem.* **2003**, *8*, 560−566.

(17) Baker, B. M.; Murphy, K. P. Dissecting the energetics of a protein-protein interaction: The binding of ovomucoid third domain to elastase. *J. Mol. Biol.* **1997**, *268*, 557−569.

(18) Fabbrizzi, L.; Micheloni, M.; Paoletti, P.; Schwarzenbach, G. Protonation processes of unusual exothermicity. *J. Am. Chem. Soc.* **1977**, *99*, 5574−5575.

(19) Goldberg, R. N.; Kishore, N.; Lennen, R. M. Thermodynamic quantities for the ionization reactions of buffers. *J. Phys. Chem. Ref. Data* **2002**, *31*, 231−370.

DOI: 10.1021/jacs.9b03512
J. Am. Chem. Soc. XXXX, XXX, XXX−XXX

(20) Berghuis, A. M.; Brayer, G. D. Oxidation state-dependent conformational changes in cytochrome *c*. *J. Mol. Biol.* **1992**, *223*, 959−976.
(21) Cherney, M. M.; Junior, C. C.; Bowler, B. E. Mutation of trimethyllysine 72 to alanine enhances His79−heme-mediated dynamics of *iso*-1-cytochrome *c*. *Biochemistry* **2013**, *52*, 837−846.
(22) Bandi, S.; Baddam, S.; Bowler, B. E. Alkaline conformational transition and gated electron transfer with a Lys 79 → His variant of iso-1-cytochrome *c*. *Biochemistry* **2007**, *46*, 10643−10654.
(23) Amacher, J. F.; Zhong, F.; Lisi, G. P.; Zhu, M. Q.; Alden, S. L.; Hoke, K. R.; Madden, D. R.; Pletneva, E. V. A compact structure of cytochrome *c* trapped in a lysine-ligated state: loop refolding and functional implications of a conformational switch. *J. Am. Chem. Soc.* **2015**, *137*, 8435−8449.
(24) Cherney, M. M.; Junior, C. C.; Bergquist, B. B.; Bowler, B. E. Dynamics of the His79-heme alkaline transition of yeast *iso*-1 cytochrome *c* probed by conformationally gated electron transfer with Co(II)bis(terpyridine). *J. Am. Chem. Soc.* **2013**, *135*, 12772−12782.
(25) Moore, G. R.; Pettigrew, G. W. *Cytochromes c: Evolutionary, Structural, and Physicochemical Aspects*; Springer-Verlag: Berlin, Germany, 1990.
(26) Pearce, L. L.; Gartner, A. L.; Smith, M.; Mauk, A. G. Mutation-induced perturbation of the cytochrome-C alkaline transition. *Biochemistry* **1989**, *28*, 3152−3156.
(27) Taniguchi, V. T.; Ellis, W. R.; Cammarata, V.; Webb, J.; Anson, F. C.; Gray, H. B. Spectroelectrochemical determination of the temperature-dependence of reduction potentials - Tris(1,10-Phenanthroline) complexes of iron and cobalt with *C*-type cytochromes. *Adv. Chem. Ser.* **1982**, *201*, 51−68.
(28) Deng, Y.; Zhong, F.; Alden, S. L.; Hoke, K. R.; Pletneva, E. V. The K79G mutation reshapes the heme crevice and alters redox properties of cytochrome *c*. *Biochemistry* **2018**, *57*, 5827−5840.
(29) Feinberg, B. A.; Liu, X.; Ryan, M. D.; Schejter, A.; Zhang, C.; Margoliash, E. Direct Voltammetric observation of redox driven changes in axial coordination and intramolecular rearrangement of the Phenylalanine-82-Histidine variant of yeast *iso*-1-cytochrome *c*. *Biochemistry* **1998**, *37*, 13091−13101.
(30) Bertrand, P.; Mbarki, O.; Asso, M.; Blanchard, L.; Guerlesquin, F.; Tegoni, M. Control of the redox potential in *c*-type cytochromes: Importance of the entropic contribution. *Biochemistry* **1995**, *34*, 11071−11079.
(31) Tezcan, F. A.; Winkler, J. R.; Gray, H. B. Effects of ligation and folding on reduction potentials of heme proteins. *J. Am. Chem. Soc.* **1998**, *120*, 13383−13388.
(32) Marvin, K. A.; Reinking, J. L.; Lee, A. J.; Pardee, K. M.; Krause, H. M.; Burstyn, J. N. Nuclear receptors *Homo sapiens* Rev-erb and *Drosophila melanogaster* E75 are thiolate-ligated heme proteins, which undergo redox-mediated ligand switching and bind CO and NO. *Biochemistry* **2009**, *48*, 7056−7071.
(33) Lan, W.; Wang, Z.; Yang, Z.; Zhu, J.; Ying, T.; Jiang, X.; Zhang, X.; Wu, H.; Liu, M.; Tan, X.; Cao, C.; Huang, Z.-X. Conformational toggling of yeast *iso*-1-cytochrome *c* in the oxidized and reduced states. *PLoS One* **2011**, *6*, No. e27219.
(34) Tang, K.; Knipp, M.; Liu, B. B.; Cox, N.; Stabel, R.; He, Q.; Zhou, M.; Scheer, H.; Zhao, K. H.; Gärtner, W. Redox-dependent ligand switching in a sensory heme-binding GAF domain of the cyanobacterium *Nostoc sp.* PCC7120. *J. Biol. Chem.* **2015**, *290*, 19067−19080.
(35) Gupta, N.; Ragsdale, S. W. Thiol-disulfide redox dependence of heme binding and heme ligand switching in nuclear hormone receptor Rev-erb*β*. *J. Biol. Chem.* **2011**, *286*, 4392−4403.

DOI: 10.1021/jacs.9b03512
J. Am. Chem. Soc. XXXX, XXX, XXX−XXX